Neoplasma 2020; 67(5): 1054–1062

doi:10.4149/neo_2020_191023N1081

LncRNA SNHG4 promotes neuroblastoma proliferation, migration, and invasion by sponging miR-377-3p

H. YANG#, J. F. GUO#, M. L. ZHANG, A. M. LI*

Department of Pediatrics, Jingzhou Central Hospital of Hubei Province, Jingzhou, Hubei, China

**Correspondence: hbjzliaimin@163.com*
#Contributed equally to this work.

Received October 23, 2019 / Accepted January 7, 2020

Long non-coding RNAs (lncRNAs) have been demonstrated to act as essential regulators in the growth and progression of neuroblastoma. In the present research, the high expression of lncRNA small nucleolar RNA host gene 4 (SNHG4) in neuroblastoma was tested via quantitative reverse transcription-polymerase chain reaction (qRT-PCR), and then the function of SNHG4 was explored and verified by CCK-8 assay, EdU assay, cell cycle assay, cell apoptosis test, wound healing test, and invasion test in neuroblastoma cell lines. It was discovered that lncRNA SNHG4 exhibited high expression in neuroblastoma tissues and cell lines, and the expression of SNHG4 was associated with the survival of neuroblastoma patients. Additionally, SNHG4 decrement markedly repressed neuroblastoma cells to proliferate and stimulate their apoptosis *in vivo* and *in vitro*. Moreover, SNHG4 decrement impeded the abilities of SH-SY5Y and IMR-32 cells to migrate and invade as well as epithelial-mesenchymal transition (EMT). In mechanism, we found that SNHG4 acted as a competing endogenous RNA to sponge miR-377-3p, which was downregulated in neuroblastomas and inhibited cell proliferation and invasion. The findings manifested that SNHG4 was inversely associated with miR-377-3p expression in neuroblastoma cases. Collectively, we revealed the functions of SNHG4 and miR-377-3p in neuroblastoma.

Key words: SNHG4, miR-377-3p, proliferation, neuroblastoma, invasion

As a heterogeneous tumor, neuroblastoma originates from neural crest progenitor cells. It is the most frequently seen solid neoplasm in children, taking up roughly 10% of all childhood cancers [1]. Its etiology is that neuronal precursor cells in the sympathetic nervous system unconventionally differentiate [2]. Neuroblastoma arises most frequently in the adrenal medulla, and also occurs in sympathetic ganglia of the sympathetic trunk and abdominal organs [3], featured with a wide range of clinical manifestations. Some patients with benign tumors undergo spontaneous regression without chemotherapy; others with metastatic disease are resistant to even intensive therapy [4, 5]. Even after intensive treatment, the survival rate of the most aggressive neuroblastoma patients is below 40% [6–8]. In recent decades, great endeavors have been made to inquire about the molecular modulating mechanisms of neuroblastoma. There is increasing evidence that lncRNAs exert crucial impacts on the growth and evolution of neuroblastoma [9, 10], but the effects of most lncRNAs in neuroblastoma are still elusive.

LncRNAs are a novel kind of RNA transcripts that are over 200 nt long and not able to encode proteins [11]. In spite of the former definition of transcriptional "noise", there are huge amounts of evidence that lncRNAs display mainstay effects in different cells and tissues [12, 13]. They have the ability to modulate cell pathophysiological activities at the epigenetic, transcriptional, or posttranscriptional levels [14–16]. New evidence suggests that lncRNAs have impacts in various human cancers, such as neuroblastoma, thyroid cancer, lung cancer, hepatocellular carcinoma [17–20]. For instance, *MEG3, linc01105,* and *HCN3* affect the proliferation and apoptosis of neuroblastoma cells through p53 and HIF-1α pathways [21]. LncRNA *H19* impedes cell viability, invasion, and migration through *IRS-1* decrement in thyroid cancer cells [22]. Hence, it is crucial to identify vital oncogenic lncRNAs for tumor diagnosis and treatment.

LncRNA *SNHG4* is 1100 bp long and located in chromosome 5q31.2. It is commonly raised in cancers and modulates cancer cells' malignant behaviors [23–25]. However, the role of *SNHG4* in neuroblastoma is unclear. In this research study, *SNHG4* evidently went up in neuroblastoma tissues relative to normal tissues. Subsequently, a train of experiments *in vitro* was executed to investigate the possible role of *SNHG4* in the

growth of neuroblastoma. To sum up, this research revealed the vital effect of the *SNHG4*/miR-377-3p axis in neuroblastoma, offering novel ideas for treating neuroblastoma.

Materials and methods

Clinical samples and cell lines. 30 neuroblastoma samples were harvested from the Jingzhou Central Hospital of Hubei Province and were verified by histopathological examination after the operation. Primary cancer tissues and paired adjacent non-cancerous tissues were immediately frozen in liquid nitrogen subsequent to resection and then stored at –80 °C prior to the extraction of RNAs. These 30 primary cancer tissues and another 30 paired adjacent non-cancerous tissues were harvested as clinical samples. This research gained the approval of the Ethics Committee of Jingzhou Central Hospital of Hubei Province.

Human neuroblastoma cell lines (SH-SY5Y, CHP-212, SK-N-FI, and IMR-32) and a human normal cell line (293T) were bought from the Type Culture Collection of Chinese Academy of Sciences (China) and American Type Culture Collection (Rockville, MD). Cell lines were authenticated by the provider, applied within 6 months after resuscitation of frozen aliquots, and cultured in RPMI 1640 medium (Life Technologies, MD) supplemented with 10% fetal bovine serum from the same company, penicillin (100 U/ml), and streptomycin (100 mg/ml). Cells were incubated in serum-free RPMI 1640 for 4 h and treatment with PJ34 (Sigma, MO) or ATRA (Sigma) complying with instructions.

RNA interference. siRNAs of *SNHG4* and siRNA-NC were provided by Sigma-Aldrich (USA). miR-377-3p mimics and NC were bought from RiboBio (China). Cells received treatment with Lipofectamine 2000 (Invitrogen) as indicated.

Cell proliferation test. CCK-8 (U-sea Biotech, China) was adopted for the examination of cell proliferation. Cells grew in 96-well plate at the density of 1×10^4 cells/well and underwent an incubation with 5% CO_2 at 37 °C until the fusion degree attained 70%. Subsequent to 48 h of plasmid treatment, the cells received continuous incubation for 1, 2, 3, 4, and 5 days, and to each well 10 μl of CCK-8 solution was added. SUNRISE Microplate Reader from Tecan (Switzerland) was utilized to measure the absorbance at 450 nm.

Apoptosis test. Flow cytometry was executed for the cell apoptosis measurement on a FACSAria flow cytometer (BD Biosciences, USA) as indicated in the protocol of the Annexin V-FITC/PI apoptosis detection kit (KeyGEN, China).

Wound healing assay and invasion experiment. Prior to the scratching of the monolayers with a pipette tip (200 μl), the cells were grown until the fusion reached 80% in the six-well plate, rinsed with PBS, and cultured in the medium with no FBS. A microscope was utilized to observe wounds, followed by photographing at 0 and 24 h.

Invasion abilities were tested with the use of the Boyden Chamber (pore size: 8 μm, BD Biosciences, USA). Then the cells were placed onto BD BioCoat Matrigel Invasion Chambers (pore size: 8 μm; BD Biosciences), and 700 μl media supplemented with 20% FBS was added to the lower chamber. Transwell membranes were fixed and stained using crystal violet after a specified time. The cells adhering to the lower surface of the membrane were counted under a light microscope (Olympus).

Reverse transcription and real-time PCR. Total RNAs were extracted from the incubated cells using Trizol reagent (Invitrogen, USA) complying with the manufacturer's regimen to synthesize cDNAs with a PrimerScript RT Reagent kit (Takara, Japan). miRNAs from total RNAs underwent RT using the Prime-Script miRNA cDNA Synthesis Kit (TaKaRa). SYBR green Premix Ex Taq II (Takara) was employed for real-time PCR on Step One Plus Real-Time PCR System (Applied Biosystems, USA). The expression level of mRNAs was detected with GAPDH as the endogenous control and miRNA expression was analyzed with U6 as the endogenous control.

***In vivo* test.** Athymic four weeks old BALB/c nude mice were kept under specific conditions free of pathogens. Then, SH-SY5Y cells were obtained and rinsed with PBS. Next, the ventral side of each mouse was subcutaneously injected with 1×10^7 cells for tumor formation experiment, and the tumor volume was checked every 7 days and calculated. The experiment gained the approval of the Animal Experiment Ethics Committee of Jingzhou Central Hospital of Hubei Province. Animal experiments took place in SPF Animal Laboratory at the Yangtze University Health Science Center.

***In vivo* lung-colonization experiment.** 1.5×10^6 of SH-SY5Y cells were injected into the tail vein of nude mice. After that, the lungs were harvested at week 9 and fixed in 10% formalin, and metastatic colonies on the lung surface were quantified with the use of a dissection microscope. All animal assays gained the approval of the Animal Care Committee of Jingzhou Central Hospital of Hubei Province and Yangtze University Health Science Center.

Luciferase reporter test. pmirGLO vector (Promega, USA) was inserted with the *SNHG4* sequence with a supposed miR-377-3p binding site that was cloned. Then cells underwent inoculation in ninety-six-well plates and the treatment with empty pmirGLO vector/recombinant plasmids and miR-377-3p mimics/NC. Subsequently, the dual luciferase reporter assay system (Promega) was employed to test the luciferase activity one day after treatment. In addition, Renilla luciferase activity was used as a normalizing control for the firefly luciferase activity detection.

Western blotting. Total proteins were extracted *via* RIPA, and SDS-PAGE gel with the appropriate concentration was selected based on the molecular weight of these proteins. Thereafter, they were transferred to a PVDF membrane followed by immunostaining. Primary antibodies (Abcam, Cambridge, MA, USA) anti-PCNA (1:1000, ab92552), anti-cyclin D1 (1:200, ab16663), anti-vimentin (1:1000, ab92547), anti-E-cadherin (1:500, ab76055) and anti-GAPDH (1:500, ab8245) were added to the membrane and incubated at 4 °C

overnight. Next, secondary antibodies (A0208 and A0216, Beyotime, Nantong, China) at the dilution ratio of 1:1000 were employed for 2 h of incubation at 37 °C, and enhanced chemiluminescence was carried out. Eventually, color development and photographing were executed.

Statistical analysis. SPSS 20.0 (IBM, SPSS, USA) and GraphPad Prism were utilized for all statistical processing, and the statistical significance in the difference between two groups or among multiple groups was detected using the Student's t-test and one-way ANOVA. Besides, correlations were determined via Pearson's correlation coefficient analysis, and the overall survival curves were plotted with the Kaplan-Meier method and were analyzed via the log-rank test. A p-value <0.05 reflected that the difference was statistically significant.

Results

***SNHG4* displays a high expression in neuroblastoma tissues and cell lines.** qRT-PCR analysis confirmed that the expression of *SNHG4* was notably elevated in neuroblastoma tissues relative to adjacent normal tissues (Figure 1A). Identically, the higher *SNHG4* expression was ascertained in neuroblastoma cell lines (Figure 1B). Thereafter, these samples were separated into *SNHG4* low-expression group and *SNHG4* high-expression group, with the median as the cutoff value. Then the survival was tested *via* Kaplan-Meier analysis, the findings of which validated that neuroblastoma patients with higher *SNHG4* expression exhibited more unfavorable survival (Figure 1C).

***SNHG4* knockdown significantly inhibits cell proliferation and induces apoptosis in neuroblastoma *in vitro* and *in vivo*.** *SNHG4* in IMR-32 and SH-SY5Y cells was reduced via si-NC and si-*SNHG4* treatment, thus inquiring the physiological roles of *SNHG4* in neuroblastoma (Figure 2A). Afterward, CCK-8 and EdU assays were implemented to determine the influence of *SNHG4* reduction on proliferation. It was discovered that *SNHG4* decrement pronouncedly impeded cells to proliferate after treatment (Figures 2B, 2C). Flow cytometry analysis (FACS) unraveled that si-SNHG4 treatment reduced the entry of SH-SY5Y and IMR-32 cells into the S phase (Figure 2D). Further, Annexin V/PI staining was implemented to examine the impacts of *SNHG4* depression on cell apoptosis, the findings of which unraveled that the *SNHG4* reduction markedly elevated the apoptosis rate of IMR-32 and SH-SY5Y cells (Figure 2E).

Assays for tumor xenografts were carried out in nude mice, so as to ascertain the role of *SNHG4* in on tumor growth *in vivo*. The tumor volume was measured every other week, and it revealed that *SNHG4* decrement strikingly delayed tumor growth *in vivo* (Figures 3A, 3B). Then the tumor weight was examined at the end of assays, and it was found that the tumor weight was pronouncedly lower in the si-SNHG4 group than in the si-NC group (Figure 3C). In addition, the protein levels of markers associated with apoptosis and proliferation in nude mice were tested through western blotting. According to the results, *SNHG4* decrement predominantly repressed the expression of markers correlated with proliferation including PCNA and Cyclin D1 but elevated the expression of proteins stimulating apoptosis such as Bax and cleaved caspase-3 (Figure 3D). Summarily, *SNHG4* decrement strikingly blocked cells to proliferate but triggered their apoptosis *in vivo* and *in vitro*.

***SNHG4* regulates neuroblastoma cell migration and invasion *in vitro* and *in vivo*.** To further determine the effects of *SNHG4* on tumor migration and invasion, we conducted wound healing and Transwell invasion assays. Results showed that the *SNHG4* knockdown significantly impaired the abilities of cell migration and invasion of SH-SY5Y and IMR-32 cells (Figures 4A, 4B). Furthermore,

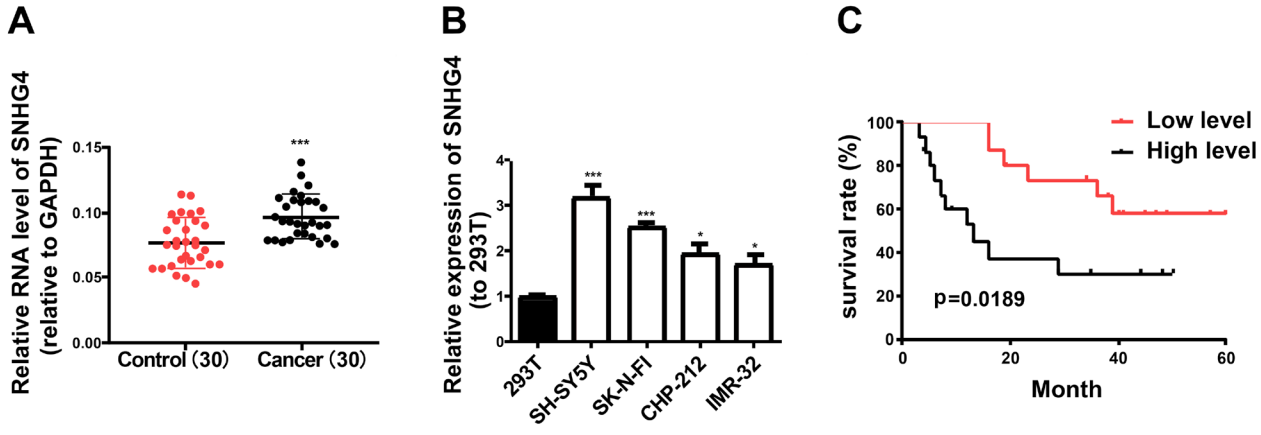

Figure 1. ***SNHG4* displays a high expression in neuroblastoma tissues and cell lines. A) Relative *SNHG4* expression was checked by qRT-PCR in neuroblastoma tissues and adjacent normal tissues. B) *SNHG4* expression was tested by qRT-PCR in neuroblastoma cell lines. C) Kaplan-Meier survival curve based on *SNHG4* expression levels. All data obtained from three individual assays are reflected as mean ± SD. *p<0.05; **p<0.01; ***p<0.001**

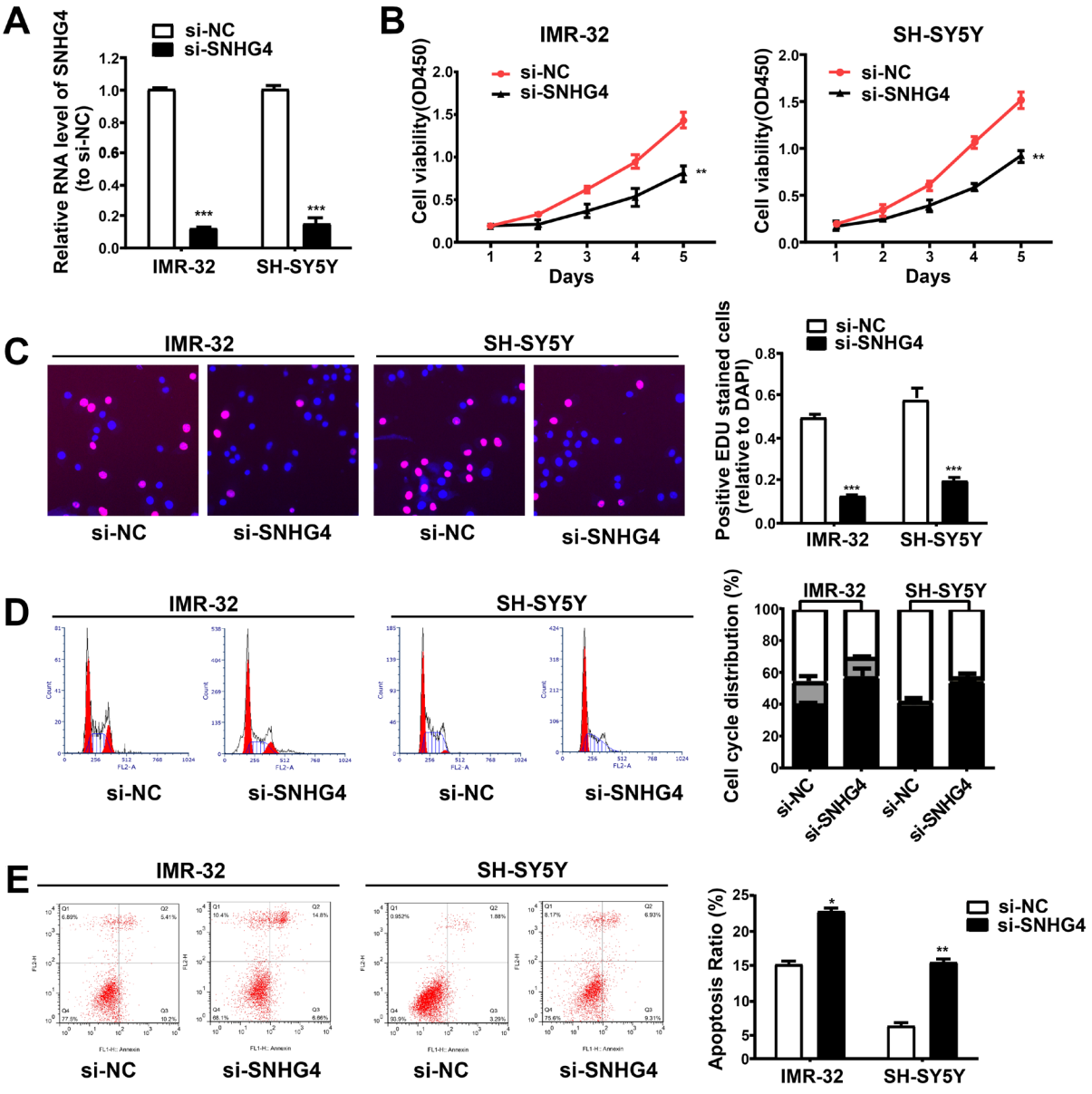

Figure 2. ***SNHG4*** **decrement significantly inhibits cell proliferation and induces apoptosis in neuroblastoma** ***in vitro*****. A)** ***SNHG4*** **expression in SH-SY5Y and IMR-32 cells treated with si-NC or si-*** ***SNHG4*** **was examined by qRT-PCR. B) The function of** ***SNHG4*** **decrement in SH-SY5Y and IMR-32 cell proliferation was tested by the CCK-8 test. C) The EdU test ascertained the functions of** ***SNHG4*** **reduction on SH-SY5Y and IMR-32 cell proliferation. D) FACS test showed that** ***SNHG4*** **decrement reduces the cells in the S phase. E) The impact of** ***SNHG4*** **reduction on SH-SY5Y and IMR-32 cell apoptosis was checked by Annexin V/PI staining. All data obtained from three individual assays are reflected as mean ± SD. *p<0.05; **p<0.01; ***p<0.001**

the knockdown of *SNHG4* can repress vimentin expression, while enhancing the E-cadherin expression in SH-SY5Y and IMR-32 cells (Figure 4C), which indicated that *SNHG4* knockdown might inhibit epithelial-mesenchymal transition in neuroblastoma. Then we checked the protein levels of tumor migration-related and invasion-related proteins (MMP2, MMP9, vimentin, SNAI1, and E-cadherin) in the formed tumor tissues of nude mice. As shown, tumor tissues derived from *SNHG4*-depleted cells had lower expression of MMP2, MMP9, SNAI1, vimentin but higher expression of E-Cadherin (Figure 4D). Furthermore, we examined the effects of *SNHG4* on lung metastasis by injecting *SNHG4* knockdown cells into nude mice *via* the lateral tail vein. After 9 weeks, we measured the nodules in the lung and found that the *SNHG4* knockdown significantly reduced the nodule number (Figure 4E). Collectively, the *SNHG4* knockdown impaired the ability of cell migration and invasion *in vitro* and *in vivo*.

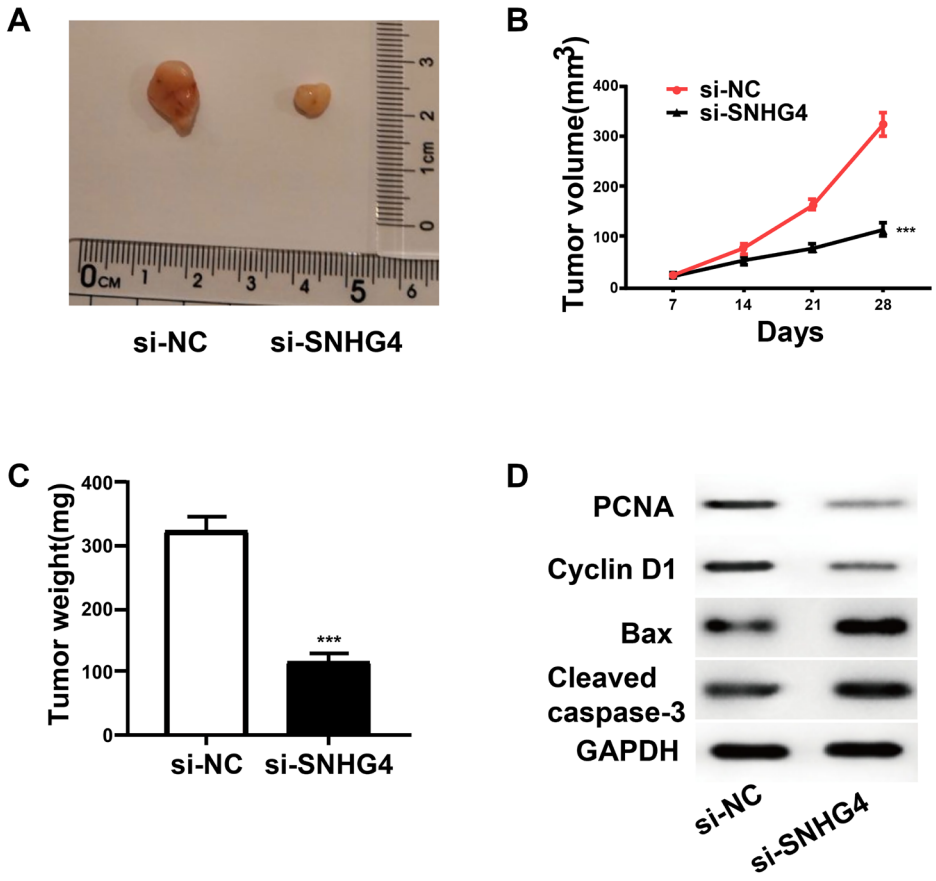

Figure 3. ***SNHG4*** **decrement strikingly represses neuroblastoma cell proliferation and triggers apoptosis** ***in vivo*****. A) Xenograft photos. B) Tumor volume was detected every other week.** ***SNHG4*** **reduction slowed down tumor growth. C) Tumor weight was determined at the end of assays. D)** ***SNHG4*** **reduction repressed PCNA and Cyclin D1 expressions but elevated cleaved caspase-3 and Bax expressions. All data obtained from three individual assays are reflected as mean ± SD. ***p<0.001**

SNHG4 **promotes neuroblastoma cell proliferation, migration, and invasion by sponging miR-377-3p.** It has been ascertained by new evidence that lncRNAs act as ceRNAs to exert their regulatory impacts [26, 27]. An online tool (http://mirdb.org/miRDB/index.html) was adopted for the prediction to continuously check the possible molecular function mechanism of *SNHG4* in neuroblastoma. The results unraveled that miR-377-3p was likely to be a target of *SNHG4*, and a possible binding site existed between miR-377-3p and *SNHG4* (Figure 5A). Subsequently, dual luciferase reporter experiments were implemented to corroborate this, and it was revealed that co-treatment with *SNHG4* WT and miR-377-3p evidently reduced 293T cell luciferase activity, and miR-377-3p mimics were not able to modulate the luciferase activity in the case of the mutation of the binding site (Figure 5B), prompting that miR-377-3p binds to *SNHG4* in a direct way. Additionally, qRT-PCR manifested that *SNHG4* expression in SH-SY5Y and IMR-32 cells was remarkably lowered by the miR-377-3p overexpression and *vice versa* (Figure 5C). And miR-377-3p expression was pronouncedly stamped down in neuroblastoma tissues (Figure 5D). What's more, an inverse relationship was found between *SNHG4* expression and miR-377-3p expression in neuroblastoma tissues (Figure 5E). Thereafter, *SNHG4* was stamped down and miR-377-3p was blocked in SH-SY5Y and IMR-32 cells for inquiring whether *SNHG4* pushed forward neuroblastoma cells to proliferate, migrate, and invade by inversely modulating miR-377-3p. EdU, CCK-8, flow cytometry, Transwell invasion, and wound healing experiments corroborated that *SNHG4* reduction notably suppressed cells to migrate, proliferate, and invade but boosted their apoptosis, which were impaired by miR-377-3p suppression (Figures 5F–5K).

Discussion

Neuroblastoma is the most common tumor in children, with a very poor prognosis [28]. Nevertheless, the possible mechanism of modulating neuroblastoma growth is essentially not clear. Advancing new molecular biomarkers for

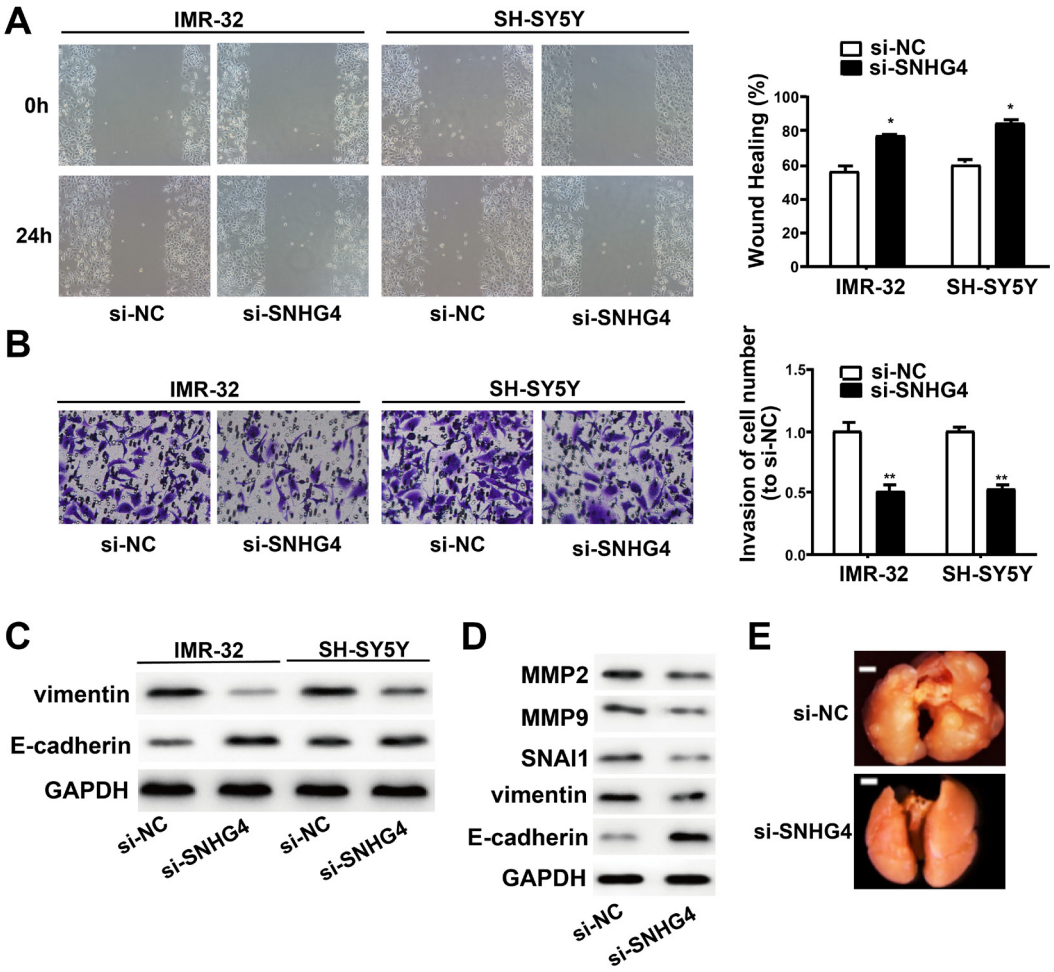

Figure 4. ***SNHG4*** **regulates neuroblastoma cell migration and invasion** ***in vitro*** **and** ***in vivo*****. A) Wound healing assay confirmed that** ***SNHG4*** **knockdown inhibited the migration of SH-SY5Y and IMR-32 cells. B) Transwell invasion test displayed that** ***SNHG4*** **reduction repressed SH-SY5Y and IMR-32 cell invasion. C) E-cadherin protein expression in SH-SY5Y and IMR-32 cells was raised but vimentin was lowered in both cells after** ***SNHG4*** **reduction. D)** ***SNHG4*** **decrement weakened cell invasion and migration capacities** ***in vivo*****. E) Pulmonary nodules at week 9. All data obtained from three individual assays are reflected as mean ± SD. *p<0.05; **p<0.01**

the diagnosis and prognosis of neuroblastoma is a pressing need. This research displayed that *SNHG4* was pronouncedly raised in neuroblastoma and it is key to neuroblastoma cell migration, proliferation, and invasion, denoting that *SNHG4* is likely to be a novel biomarker for neuroblastoma. Nevertheless, given the relatively big difference in SNHG4 expression levels in IMR-32 and SH-SY5Y cells, it is intriguing that some si-NC/miR-NC control data in these two cell lines are quite similar, for example, the cell viability. This phenomenon means that there are some other factors involved in cell migration, proliferation, and invasion of different neuroblastoma cell lines. In the future study, we would further explore these factors.

Previous evidence corroborated that lncRNAs sponged miRNAs as ceRNAs [29, 30]. In the present research, speculation was made to continuously inquire about the possible molecular regulatory mechanism of *SNHG4* in neuroblastoma, and the findings unraveled that miR-377-3p was an underlying candidate. It has been ascertained that miR-377-3p functions in different cancer cells. For example, *LINC00339* promotes gastric cancer evolution by raising *DCP1A* expression via miR-377-3p repression [31]. Besides, miR-377-3p represses growth and invasion through sponging *JAG1* in ovarian cancer [32]. The research above denotes that miR-377-3p is likely to be a tumor suppressor. But miR-377-3p's role in neuroblastoma is still unclear currently. In the present research, miR-377-3p was stamped down in neuroblastoma tissues. Luciferase reporter experiment corroborated that *SNHG4* binds to miR-377-3p in a direct way. Additionally, EdU, CCK-8, flow cytometry, Transwell invasion, and wound healing experiments were excised to continuously check whether *SNHG4* booted cells to migrate,

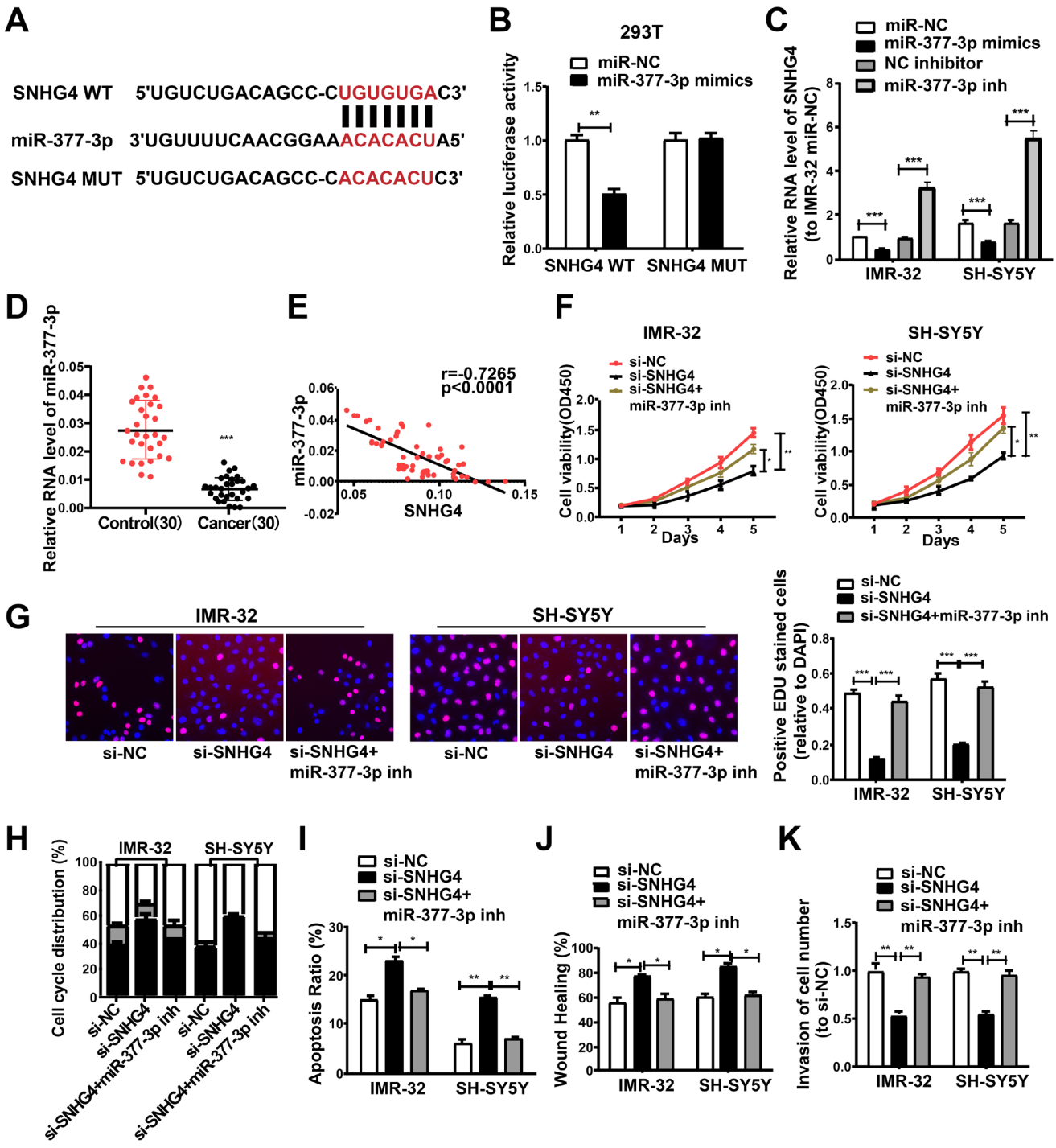

Figure 5. ***SNHG4*** **promotes neuroblastoma cell proliferation, migration, and invasion by sponging miR-377-3p. A) Bioinformatics analysis was executed to forecast the miR-377-3p binding sites in** ***SNHG4****. B) Luciferase reporter tests were implemented using 293T cells co-treated with the miR-377-3p mimics/miR-NC and* ***SNHG4****-WT/Mut reporter plasmid. C) Relative qRT-PCR assessment unraveled that miR-377-3p overexpression notably lowered* ***SNHG4*** **level in SH-SY5Y and IMR-32 cells and** ***vice versa****. D) miR-377-3p expression level was checked* ***via*** **qRT-PCR in neuroblastoma and paired adjacent non-cancerous tissues. E) The inverse relationship between** ***SNHG4*** **and miR-377-3p expression levels was measured in 30 neuroblastoma tissues. F, G) CCK-8 and EdU tests manifested that** ***SNHG4*** **decrement blocked SH-SY5Y and IMR-32 cells to proliferate, which was reversed by the miR-377-3p repression. H)** ***SNHG4*** **knockdown inhibited cell cycle whereas miR-377-3p repression in the meantime reversed it. I)** ***SNHG4*** **reduction stimulated cell apoptosis while miR-377-3p repression reversed it. J, K) Wound healing assay and Transwell invasion experiment suggested that** ***SNHG4*** **decrement blocks SH-SY5Y and IMR-32 cells to migrate and invade, which was reversed by miR-377-3p repression. All data obtained from three individual assays are reflected as mean ± SD. *p<0.05; **p<0.01; ***p<0.001**

proliferate, and invade through miR-377-3p repression. The findings ascertained that functions of *SNHG4* decrement in cell migration, proliferation, and invasion were turned down by miR-377-3p repression.

To sum up, research findings displayed that the oncogene *SNHG4* contributed to the evolution of neuroblastoma by inverse modulation on miR-377-3p that repressed the tumor. Besides, *SNHG4*/miR-377-3p is likely to function as a new target for treating neuroblastoma.

References

[1] ZHUO ZJ, ZHANG R, ZHANG J, ZHU J, YANG T et al. Associations between lncRNA MEG3 polymorphisms and neuroblastoma risk in Chinese children. Aging (Albany NY) 2018; 10: 481–491. https://doi.org/10.18632/aging.101406

[2] PANDEY GK, MITRA S, SUBHASH S, HERTWIG F, KANDURI M et al. The risk-associated long noncoding RNA NBAT-1 controls neuroblastoma progression by regulating cell proliferation and neuronal differentiation. Cancer Cell 2014; 26: 722–737. https://doi.org/10.1016/j.ccell.2014.09.014

[3] BRODEUR GM. Neuroblastoma: biological insights into a clinical enigma. Nat Rev Cancer 2003; 3: 203–216. https://doi.org/10.1038/nrc1014

[4] CHEUNG NK, DYER MA. Neuroblastoma: developmental biology, cancer genomics and immunotherapy. Nat Rev Cancer 2013; 13: 397–411. https://doi.org/10.1038/nrc3526

[5] MACFARLAND S, BAGATELL R. Advances in neuroblastoma therapy. Curr Opin Pediatr 2019; 31: 14–20. https://doi.org/10.1097/MOP.0000000000000711

[6] HISHIKI T, FUJINO A, WATANABE T, TAHARA K, OHNO M et al. Definitive Tumor Resection after Myeloablative High Dose Chemotherapy Is a Feasible and Effective Option in the Multimodal Treatment of High-Risk Neuroblastoma: A Single Institution Experience. J Pediatr Surg 2019. https://doi.org/10.1016/j.jpedsurg.2019.08.050

[7] ESPOSITO MR, AVEIC S, SEYDEL A, TONINI GP. Neuroblastoma treatment in the post-genomic era. J Biomed Sci 2017; 24: 14. https://doi.org/10.1186/s12929-017-0319-y

[8] MATTHAY KK, MARIS JM, SCHLEIERMACHER G, NAKAGAWARA A, MACKALL CL et al. Neuroblastoma. Nat Rev Dis Primers 2016; 2: 16078. https://doi.org/10.1038/nrdp.2016.78

[9] WANG H, LIAO S, LI H, CHEN Y, YU J. Long Non-coding RNA TUG1 Sponges Mir-145a-5p to Regulate Microglial Polarization After Oxygen-Glucose Deprivation. Front Mol Neurosci 2019; 12: 215. https://doi.org/10.3389/fnmol.2019.00215

[10] LI D, WANG X, MEI H, FANG E, YE L et al. Long Noncoding RNA pancEts-1 Promotes Neuroblastoma Progression through hnRNPK-Mediated beta-Catenin Stabilization. Cancer Res 2018; 78: 1169–1183. https://doi.org/10.1158/0008-5472.CAN-17-2295

[11] MISAWA A, TAKAYAMA K, URANO T, INOUE S. Androgen-induced Long Noncoding RNA (lncRNA) SOCS2-AS1 Promotes Cell Growth and Inhibits Apoptosis in Prostate Cancer Cells. J Biol Chem 2016; 291: 17861–17880. https://doi.org/10.1074/jbc.M116.718536

[12] CHEN T, XIE W, XIE L, SUN Y, ZHANG Y et al. Expression of long noncoding RNA lncRNA-n336928 is correlated with tumor stage and grade and overall survival in bladder cancer. Biochem Biophys Res Commun 2015; 468: 666–670. https://doi.org/10.1016/j.bbrc.2015.11.013

[13] JIANG X, YAN Y, HU M, CHEN X, WANG Y et al. Increased level of H19 long noncoding RNA promotes invasion, angiogenesis, and stemness of glioblastoma cells. J Neurosurg 2016; 124: 129–136. https://doi.org/10.3171/2014.12.JNS1426

[14] TERASHIMA M, ISHIMURA A, WANNA-UDOM S, SUZUKI T. MEG8 long noncoding RNA contributes to epigenetic progression of the epithelial-mesenchymal transition of lung and pancreatic cancer cells. J Biol Chem 2018; 293: 18016–18030. https://doi.org/10.1074/jbc.RA118.004006

[15] SALLAM T, JONES M, THOMAS BJ, WU X, GILLILAND T et al. Transcriptional regulation of macrophage cholesterol efflux and atherogenesis by a long noncoding RNA. Nat Med 2018; 24: 304–312. https://doi.org/10.1038/nm.4479

[16] RAVEENDRA BL, SWARNKAR S, AVCHALUMOV Y, LIU XA, GRINMAN E et al. Long noncoding RNA GM12371 acts as a transcriptional regulator of synapse function. Proc Natl Acad Sci U S A 2018; 115: E10197–E10205. https://doi.org/10.1073/pnas.1722587115

[17] JING H, QU X, LIU L, XIA H. A Novel Long Noncoding RNA (lncRNA), LL22NC03-N64E9.1, Promotes the Proliferation of Lung Cancer Cells and is a Potential Prognostic Molecular Biomarker for Lung Cancer. Med Sci Monit 2018; 24: 4317–4323. https://doi.org/10.12659/MSM.908359

[18] FU XM, GUO W, LI N, LIU HZ, LIU J et al. The expression and function of long noncoding RNA lncRNA-ATB in papillary thyroid cancer. Eur Rev Med Pharmacol Sci 2017; 21: 3239–3246.

[19] GUO Z, ZHANG J, FAN L, LIU J, YU H et al. Long Noncoding RNA (lncRNA) Small Nucleolar RNA Host Gene 16 (SNHG16) Predicts Poor Prognosis and Sorafenib Resistance in Hepatocellular Carcinoma. Med Sci Monit 2019; 25: 2079–2086. https://doi.org/10.12659/MSM.915541

[20] ZHAO X, LI D, HUANG D, SONG H, MEI H et al. Risk-Associated Long Noncoding RNA FOXD3-AS1 Inhibits Neuroblastoma Progression by Repressing PARP1-Mediated Activation of CTCF. Mol Ther 2018; 26: 755–773. https://doi.org/10.1016/j.ymthe.2017.12.017

[21] TANG W, DONG K, LI K, DONG R, ZHENG S. MEG3, HCN3 and linc01105 influence the proliferation and apoptosis of neuroblastoma cells via the HIF-1alpha and p53 pathways. Sci Rep 2016; 6: 36268. https://doi.org/10.1038/srep36268

[22] ZHAO JH, SUN JX, SONG YX, CHEN XW, YANG YC et al. A novel long noncoding RNA-LOWEG is low expressed in gastric cancer and acts as a tumor suppressor by inhibiting cell invasion. J Cancer Res Clin Oncol 2016; 142: 601–609. https://doi.org/10.1007/s00432-015-2071-6

[23] TANG Y, WU L, ZHAO M, ZHAO G, MAO S et al. LncRNA SNHG4 promotes proliferation, migration, invasion and epithelial-mesenchymal transition of lung cancer cells by regulating miR-98-5p. Biochem Cell Biol 2019; 97: 767–776. https://doi.org/10.1139/bcb-2019-0065

[24] JI N, WANG Y, BAO G, YAN J, JI S. LncRNA SNHG14 promotes the progression of cervical cancer by regulating miR-206/YWHAZ. Pathol Res Pract 2019; 215: 668–675. https://doi.org/10.1016/j.prp.2018.12.026

[25] XU R, FENG F, YU X, LIU Z, LAO L. LncRNA SNHG4 promotes tumour growth by sponging miR-224-3p and predicts poor survival and recurrence in human osteosarcoma. Cell Prolif 2018; 51: e12515. https://doi.org/10.1111/cpr.12515

[26] CHEN W, PENG R, SUN Y, LIU H, ZHANG L et al. The topological key lncRNA H2k2 from the ceRNA network promotes mesangial cell proliferation in diabetic nephropathy via the miR-449a/b/Trim11/Mek signaling pathway. FASEB J 2019; 33: 11492–11506. https://doi.org/10.1096/fj.201900522R

[27] WANG C, CHEN Y, WANG Y, LIU X, LIU Y et al. Inhibition of COX-2, mPGES-1 and CYP4A by isoliquiritigenin blocks the angiogenic Akt signaling in glioma through ceRNA effect of miR-194-5p and lncRNA NEAT1. J Exp Clin Cancer Res 2019; 38: 371. https://doi.org/10.1186/s13046-019-1361-2

[28] CHEN G, CHEN W, YE M, TAN W, JIA B. TRIM59 knockdown inhibits cell proliferation by down-regulating the Wnt/beta-catenin signaling pathway in neuroblastoma. Biosci Rep 2019; 39: BSR20181277. https://doi.org/10.1042/BSR20181277

[29] WANG LX, WAN C, DONG ZB, WANG BH, LIU HY et al. Integrative Analysis of Long Noncoding RNA (lncRNA), microRNA (miRNA) and mRNA Expression and Construction of a Competing Endogenous RNA (ceRNA) Network in Metastatic Melanoma. Med Sci Monit 2019; 25: 2896–2907. https://doi.org/10.12659/MSM.913881

[30] PENG W, DENG W, ZHANG J, PEI G, RONG Q et al. Zhu S. Long noncoding RNA ANCR suppresses bone formation of periodontal ligament stem cells via sponging miRNA-758. Biochem Biophys Res Commun 2018; 503: 815–821. https://doi.org/10.1016/j.bbrc.2018.06.081

[31] SHI C, LIU T, CHI J, LUO H, WU Z et al. LINC00339 promotes gastric cancer progression by elevating DCP1A expression via inhibiting miR-377-3p. J Cell Physiol 2019; 234: 23667–23674. https://doi.org/10.1002/jcp.28934

[32] LIU Y, LIU B, LIU Y, CHEN S, YANG J et al. MicroRNA expression profile by next-generation sequencing in a novel rat model of contrast-induced acute kidney injury. Ann Transl Med 2019; 7: 178. https://doi.org/10.21037/atm.2019.04.44